Original Article

Cervical artery tortuosity—a reliable semi-automated magnetic resonance-based method

Lukas Mayer-Suess[1]^, Tamara Peball[1], Sergiy Pereverzyev Jr[2,3], Ruth Steiger[2,3], Malik Galijasevic[2,3], Stefan Kiechl[1,4], Michael Knoflach[1,4], Elke R. Gizewski[2,3], Stephanie Mangesius[2,3]^

[1]Department of Neurology, Medical University of Innsbruck, Innsbruck, Austria; [2]Department of Neuroradiology, Medical University of Innsbruck, Innsbruck, Austria; [3]Neuroimaging Research Core Facility, Medical University of Innsbruck, Innsbruck, Austria; [4]VASCage, Research Centre on Clinical Stroke Research, Innsbruck, Austria

Contributions: (I) Conception and design: L Mayer-Suess, M Knoflach, ER Gizewski; (II) Administrative support: L Mayer-Suess, R Steiger, T Peball; (III) Provision of study materials or patients: L Mayer-Suess, M Knoflach, ER Gizewski; (IV) Collection and assembly of data: L Mayer-Suess, T Peball; (V) Data analysis and interpretation: L Mayer-Suess, S Mangesius, S Pereverzyev Jr; (VI) Manuscript writing: All authors; (VII) Final approval of manuscript: All authors.

Correspondence to: Stephanie Mangesius, MD, PhD; Sergiy Pereverzyev Jr, MSc, PhD. Department of Neuroradiology, Medical University of Innsbruck, Anichstraße 35, A-6020 Innsbruck, Austria; Neuroimaging Research Core Facility, Medical University of Innsbruck, Innsbruck, Austria. Email: Stephanie.Mangesius@i-med.ac.at; sergiy.pereverzyev@i-med.ac.at.

Background: Assessments of subclinical connective tissue disorders depend on complex approaches, emphasizing the need for more accessible methods applicable to clinical routine. Therefore, we aimed to establish a reliable approach assessing cervical vessel tortuosity, which is known to be associated with such disorders.

Methods: Magnetic resonance angiography (MRA) images of ReSect study participants [single-center prospective cohort of spontaneous cervical artery dissection (sCeAD) patients] were used. Each patient underwent the same magnetic resonance imaging (MRI) protocol. The segmentation procedure was done using MATrix LABoratory 9.4 [up-sampling of raw MRA images, distance metric (DM) calculation], ITK-SNAP [region of interest (ROI) determination, vessel segmentation] and Vascular Modelling ToolKit (centerline determination). To assess inter-user variability and validity, we (I) had two blinded independent users segment all arteries and we (II) compared the results of our method to visual appraisal of vessel tortuosity done by two blinded expert neuro-radiologists.

Results: A total of 526 extracranial cervical arteries were available for analysis. The inter-user variability of our method users was below 0.5% throughout. Overall, our method outperformed the visual tortuosity appraisal, as the visual grading underestimated the DM in 38.8% subjects when tasked to assess overall cervical artery tortuosity (both vertebral and internal carotid arteries) and in 16.6% and 33.3% respectively if tasked to grade anterior or posterior circulation separately.

Conclusions: We present a reliable method to assess cervical artery tortuosity derived from MRA images applicable in clinical routine and future research investigating the potential correlation of sCeAD and connective tissue disorder.

Keywords: Vertebral artery (VA); carotid artery; internal; dissection; magnetic resonance imaging (MRI)

Submitted Jul 26, 2023. Accepted for publication Nov 09, 2023. Published online Jan 02, 2024.
doi: 10.21037/qims-23-1057
View this article at: https://dx.doi.org/10.21037/qims-23-1057

^ ORCID: Lukas Mayer-Suess, 0000-0002-2856-0101; Stephanie Mangesius, 0000-0001-5790-2724.

Introduction

Subclinical connective tissue disorders have long been a topic of interest concerning the pathophysiology of spontaneous cervical artery dissection (sCeAD) (1-4). As clinical stigmata of connective tissue disorder are undependable, today's assessment of these underlying conditions depend on complex analyses, such as proteomics-based approaches (2,5). Therefore, there is obvious need for more readily available and easy to use biomarkers to, for instance, identify patients at risk of dissection recurrence on a long-run. Arterial tortuosity, defined by elongation and increased twisting and turning of arterial vessels, is known to be increased in hereditary connective tissue disorders with higher tortuosity indices directly correlating to the probability of arterial dissection in such patients (6-10). Therefore, we aimed to establish a reliable method to assess extracranial vessel tortuosity.

Methods

The study was conducted in accordance with the Declaration of Helsinki (as revised in 2013). The study was approved by the institutional ethics committee of the Medical University of Innsbruck (EK#UN5072;325/4.1) and all patients provided appropriate informed consent.

Patient cohort

A sub-sample of the ReSect study was used to establish our imaging methodology (2,11,12). In short, the ReSect study is a prospective cohort study and primarily consists of patients with sCeAD treated at the Medical University of Innsbruck between 1996 and 2016. For study inclusion, dissection related intramural hematoma in T1-weighted fat-saturated magnetic resonance imaging (MRI) was mandatory for each patient. During a study-specific in-house visit, a 3-Tesla contrast-enhanced MRI was performed, using the step-by-step process as listed below. Additionally, healthy controls without pre-existing cerebro- or cardiovascular disease were collected within the ReSect study.

Imaging methodology

MRI was performed on the Neuroimaging Research Core Facility, which is a 3-Tesla whole body system (Verio, Siemens, Erlangen, Germany) employing a 12-channel head coil, a neck-coil and a large flex body array coil, each consecutively covering brain, neck, torso and pelvis. All patients were scanned head first in the supine position. Every subject underwent a whole brain MRI for structural clarification. For the arterial magnetic resonance angiography (MRA, Angio3D), standard procedure 3D MRA was performed. In short, the same flash 3D sequence was acquired twice, one before and one after contrast agent injection. For each patient, two overlapping 3D imaging blocks were coronal attained, one covering the anatomical area from top of the brain to the aortic arch and the second part from there on downwards to the aortic bifurcation. As contrast-enhanced MRA is very sensitive to contrast arrival in the region of interest (ROI), two different timings of bolus injections were operated, for each imaging block, respectively.

Segmentation and analysis

The raw MRA images were first up-sampled using MATrix LABoratory (MATLAB) 9.4 (The MathWorks, Natick, MA, USA). Vessel segmentation was performed using the up-sampled MRA-imaging data of all cervical arteries using ITK-SNAP (http://www.itksnap.org/) (13). The segmentation procedure in ITK-SNAP consists of the following steps.

(I) ROI determination

An example for the following procedure is depicted in *Figure 1*. First, as the ROI corresponds to a rectangular cuboid in ITK-SNAP, we determined the coordinates of its corners (*Figure 1A*). To define these coordinates, the axial view of our up-sampled MRA images was used (*Figure 1B*). Then, to identify a start- (y_{max}) and end-point (y_{min}), the artery was visually traced to the point of exit from the corresponding proximal or distal vessel. The cursor inspector in ITK-SNAP consequently delivers the y_{max} and y_{min} coordinates (*Figure 1C*). To obtain x_{min} and z_{min} values, we began by using the y_{min} slice of the MRA images and applied the ITK-SNAP cursor, which divides each slice into four rectangles. A user then continuously traced the studied artery downwards towards y_{max} and consequently modified the cursor position so that the studied vessel remained in the lower left rectangle (*Figure 1D*, panel D1). The final cursor position delivered x_{min} and z_{min}. The last coordinates, x_{max} and z_{max}, are obtained in the same way, but the studied artery had to remain in the upper right rectangle of the ITK-SNAP cursor (*Figure 1D*, panel D2).

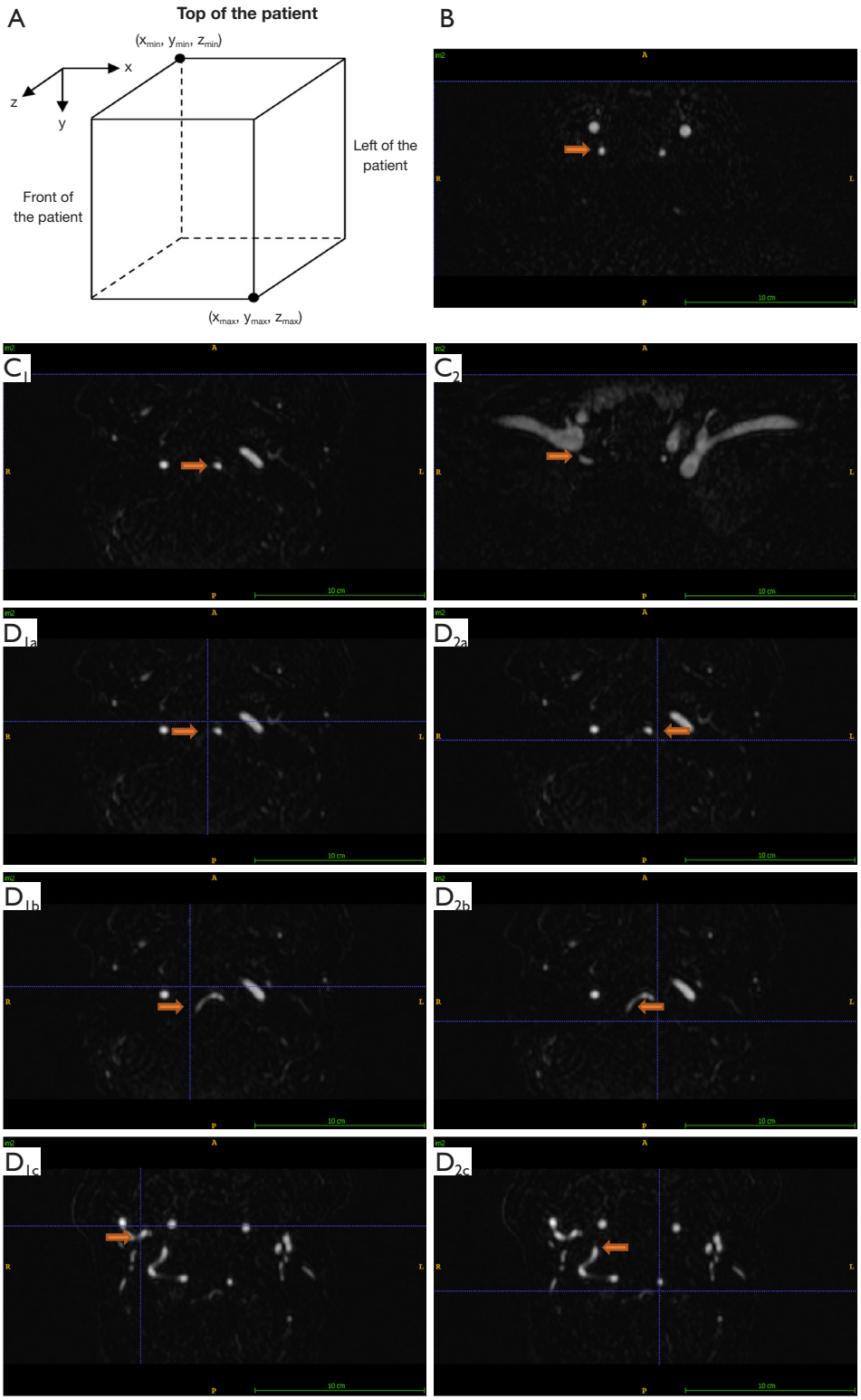

Figure 1 Determination of the ROI. (A) Schematic illustration of ROI cuboid; (B) identification of studies artery; (C) definition of start and end-point (y_{max}, y_{min}) coordinates of the artery; (D) cuboid side characterization (x_{min}/z_{min} and x_{max}/z_{max}). The red arrows highlight the artery of interest currently being analyzed. ROI, region of interest.

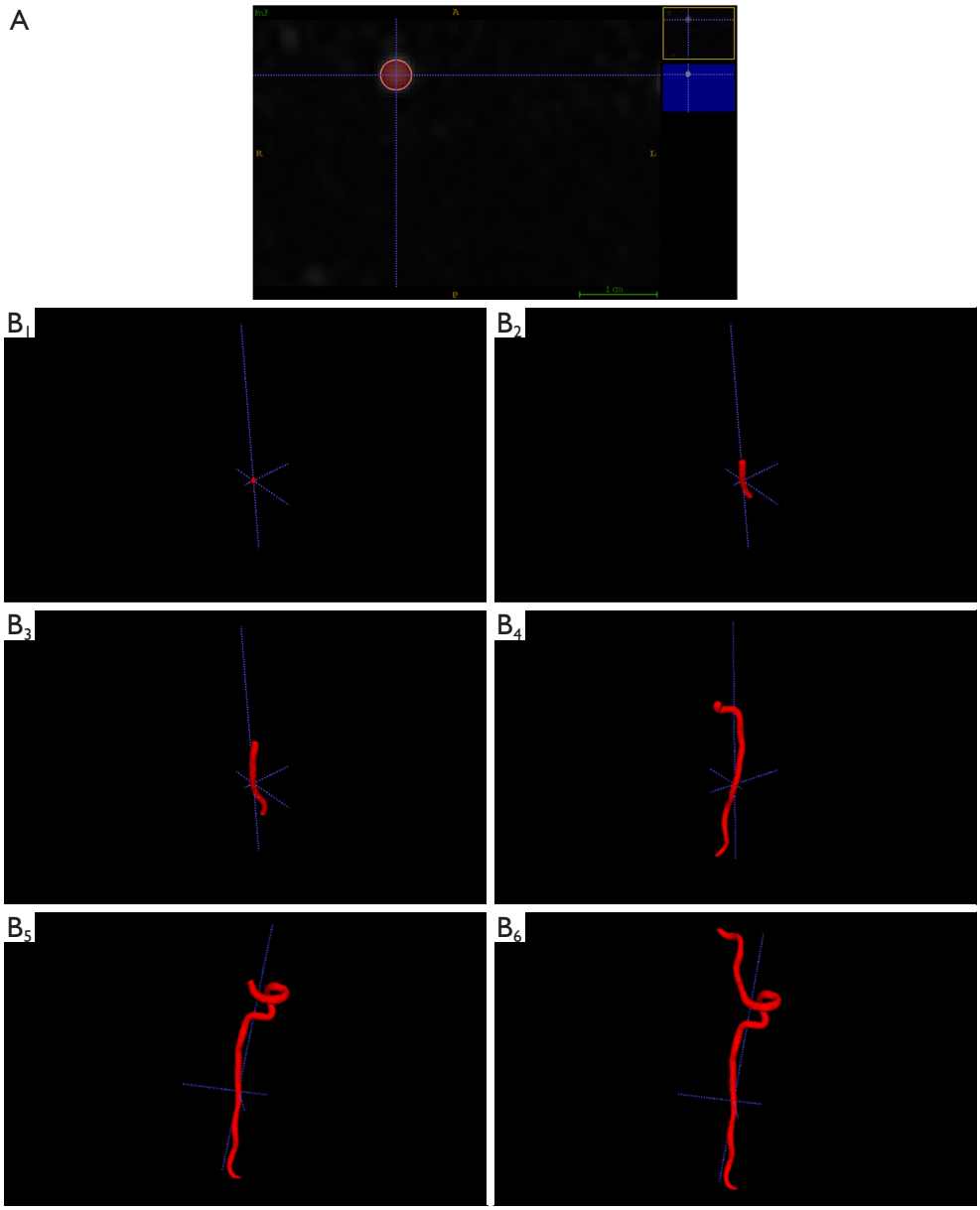

Figure 2 Initiation and progression of vessel segmentation within the ROI using ITK-SNAP. (A) First bubble set manually in studied artery; (B) automatic progression of vessel segmentation. ROI, region of interest.

(II) Segmentation

Still using ITK-SNAP, the segmentation is initiated by activating the Active Contour (Snake) Segmentation Mode. After inserting the aforementioned ROI parameters, 3D segmentation can be started. First, after selecting the Threshold mode in ITK-SNAP, the "Lower threshold only" option is to be selected. ITK-SNAP subsequently delivers the automatic segmentation threshold (AST) value, which derives from the distribution of intensity values in the ROI. In vertebral arteries, due to the smaller diameter, we chose a corrected AST (AST ×0.75). Next, the AST is set as the lower threshold. Consequently, the cursor is set in the center of the investigated artery and, with the bubble radius set at 2, a bubble is added at the cursor (*Figure 2A*). "Continuous Update Option" is selected and run, which initiates the segmentation in a 3D-view (*Figure 2B*). If the artery is fully

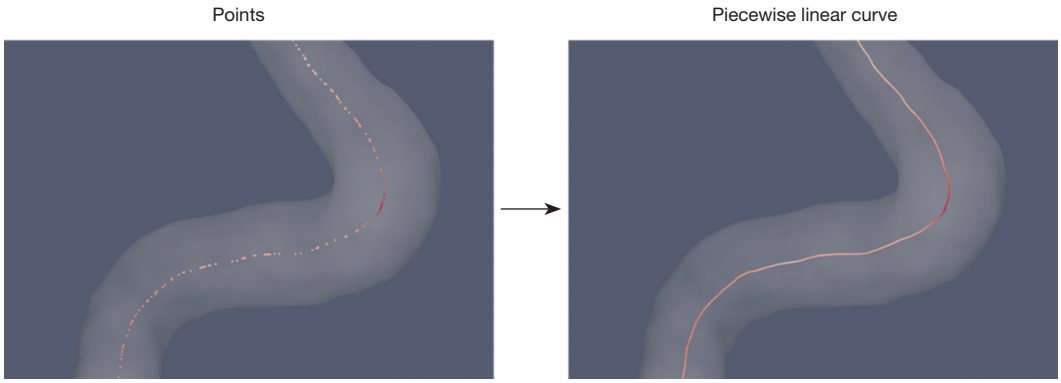

Figure 3 Centerline generated by VMTK. VMTK, Vascular Modeling Toolkit.

segmented, the data can be exported as surface mesh. If not, an additional segmentation is done by reapplying the above-mentioned steps the attain ROI values but only containing the unsegmented part of the artery and either smaller correction of the AST (e.g., AST ×0.5) is needed or manual segmentation correction via the paintbrush tool is done.

(III) Centerline determination

The centerline of the studied artery is determined through the Vascular Modeling Toolkit (VMTK) (http://www.vmtk.org/; version 1.4.0). In VMTK, we highlight the beginning and end of the segmented artery. Thereafter, the centerline is computed. We refer to (http://www.vmtk.org/tutorials/Centerlines.html) for the technical details. In the data supplement, in the file "vmtk.txt" (https://cdn.amegroups.cn/static/public/qims-23-1057-vmtk.txt), we present the employed by use VMTK commands (data supplement 1: vmtk.txt; https://cdn.amegroups.cn/static/public/qims-23-1057-vmtk.txt). VMTK generates the centerline as a sequence of points with the coordinates (x_i, y_i, z_i), $i = 1,..., N$ (*Figure 3*).

(IV) Distance metric (DM) calculation

The DM is the ratio between the length following said centerline and the straight-line distance between its two endpoints. Assuming that the centerline is a piecewise linear curve with the knots (x_i, y_i, z_i) , the DM is then calculated by the following formula:

$$DM = \frac{\sum_{i=1}^{N-1} \sqrt{(x_{i+1}-x_i)^2 + (y_{i+1}-y_i)^2 + (z_{i+1}-z_i)^2}}{\sqrt{(x_N-x_1)^2 + (y_N-y_1)^2 + (z_N-z_1)^2}} \quad [1]$$

The scripts that are used in our method can be found in the data supplement (data supplement 2: main.m; https://cdn.amegroups.cn/static/public/qims-23-1057-main.m).

Validation

To assess reproducibility and validity, a two-step validation process was performed. First, all vessels of each included subject were segmented by two blinded independent users, both being inexperienced in neurovascular anatomy or neuro-radiological imaging interpretation, to assess inter-user variability of our methodology. The second step included a two-part visual appraisal of vessel tortuosity using 3D rotatable maximum intensity projection images of the MRA done by two blinded expert neuro-radiologists (S.M. and E.R.G.), which to-date is considered the gold standard of tortuosity interpretation. Both visual graders received the identical subset of subjects. Initially, both graders were tasked to allocate 18 subjects concerning their overall impression of cervical artery tortuosity into three groups: (I) no tortuosity; (II) medium tortuosity; and (III) high tortuosity. The selection process for these subjects consisted of splitting the DM values obtained through our method and picking subjects with all four cervical arteries in either the first-, second-, or third-DM value tertile at random. Lastly, both graders were tasked to do the same but only grading the anterior or posterior circulation in six subjects respectively (i.e., 12 total).

Variable definitions

Tortuosity

Tortuosity was assessed through the DM, with the DM being the ratio between the real length (along the center line) of the vessel and the straight-line distance between the start- and endpoint of the vessel.

Figure 4 Examples of segmented VA and the corresponding centerline for one patient. VA, vertebral artery.

Table 1 Inter-user variability in percent between two raters for the DM

Cervical arteries	Right	Left
VA (%)	0.0881±0.1955	0.1055±0.1174
ICA (%)	0.2057±0.4056	0.1548±0.1709

Values are given in mean ± standard deviation. DM, distance metric; VA, vertebral artery; ICA, internal carotid artery.

Results

Cohort

In total, 174 individuals, 148 patients with sCeAD and 26 healthy controls, took part in the ReSect study. After excluding those without magnetic resonance (MR) (i.e., due to agoraphobia), data of 249 vertebral artery (VA) and 277 internal carotid artery (ICA) MRAs were used to establish our methodology.

Vessel segmentation

Through our step-wise method explained in detail in the methods section a total of 526 arteries were segmented. Examples of segmented vessels are given in *Figure 4*.

Table 2 Visual ratings through grade system of cervical arteries with 1 being low and 3 being high tortuosity

Subject	Segmentation tertile	Visual rater 1	Visual rater 2
Subject 1	1	1	1
Subject 2	1	1	1
Subject 3	1	1	1
Subject 4	1	1	1
Subject 5	1	1	1
Subject 6	1	1	1
Subject 7	2†	1†	1†
Subject 8	2	2	2
Subject 9	2	2	2
Subject 10	2†	1†	1†
Subject 11	3	3	3
Subject 12	3	3	3
Subject 13	3	3	3
Subject 14	3†	2†	2†
Subject 15	3†	2†	2†
Subject 16	3†	2†	2†
Subject 17	3†	2†	2†
Subject 18	3†	2†	2†

†, underestimated subjects.

Inter-user variability of segmentation

Table 1 depicts the inter-user variability of DM values of individual cervical arteries between the two neuro-anatomically inexperienced raters. Throughout all measurements, the inter-user variability remained below 1% and was especially low for vertebral arteries. No marked side-by-side difference could be reported.

Clinical applicability—overall visual grading of all cervical arteries

The results of the first round are given in *Table 2*. In short, both experienced neuroradiologists correctly attributed increased tortuosity to each patient and graded tortuosity in every subject identically. In comparison to our method however, the gold standard of tortuosity interpretation (visual grading by experienced neuroradiologists) underestimated the tortuosity in 7 of the 18 (38.9%)

Table 3 Visual ratings of anterior and posterior circulation separately

Subjects based on circulation	Segmentation tertile	Visual rater 1	Visual rater 2
Anterior circulation			
Subject 1	1	1	1
Subject 2	1	1	1
Subject 3	2	2	2
Subject 4	2†	1†	1†
Subject 5	3	3	3
Subject 6	3	3	3
Posterior circulation			
Subject 1	1‡	2‡	2‡
Subject 2	1	1	1
Subject 3	2†	1†	1†
Subject 4	2	2	2
Subject 5	3	3	3
Subject 6	3	3	3

†, underestimated subjects; ‡, overestimated subjects.

subjects when having to give an overall opinion of all four cervical arteries.

Clinical applicability—individual grading of all anterior and posterior circulation

The above-mentioned difference between visual grading and our method of tortuosity assessment remained when neuroradiologists were tasked with solely grading the anterior or posterior circulation or anterior circulation separately. One of 6 (16.7%) of anterior and 2 of 6 (33.3%) of posterior circulation subjects tortuosity was different in visual rating compared to our vessel segmentation measurement (*Table 3*).

Discussion

Neuro-radiological assessments of the cervico-cerebral vasculature are becoming more elaborate over time. Increased cervical artery tortuosity can for one pose an issue in acute management of stroke patients due to the more complicated passage of micro-catheters in endovascular thrombectomy but has recently additionally been discussed used as a potential biomarker in neurovascular research. Therefore, the necessity for reliable methods to objectively assess cerebrovascular images in the future is clear. One example, which has become a topic of interest recently, is extracranial vessel tortuosity, especially in patients with sCeAD (14,15). Previous studies of cervical artery tortuosity, however, mostly depended on 2D-analysis of contrast enhanced computer tomography- or MR-images, hampering the validity of tortuosity measures which heavily depend on 3D-assessment. Therefore, we present an optimized method, including additional self-improved scripts with the following key strengths: First, it is reliable, as the inter-user-variability of DM values in two independent users, inexperienced in neurovascular anatomy or neuro-radiological imaging interpretation who segmented 526 individual cervical arteries, was below 0.5% throughout. Second, it delivers more detailed measures of vascular tortuosity compared to visual rating by experienced neuro-radiologists. Even though our visual raters were in line with our segmentation method concerning the yes or no answer of vascular tortuosity being present in almost all of the cases, they were less likely to adequately differentiate between medium and high-grade tortuosity, especially if they were tasked to give an overall assessment of all cervical arteries. When addressing possible limitations of our method, segmentation errors and definition of start- and end-points of segmented arteries were the most pressing. These initial road-blocks could adequately be accounted for through our in-house developed standard operating procedures and MATLAB scripts, which is emphasized by our inter-user variability measurement. Lastly, applicability to larger cohorts has yet to be proven, but is highly probable due to the previously elaborated usability and low inter-user variability of unexperienced users.

Conclusions

We present a reliable method to assess cervical artery tortuosity derived from MRA images applicable in clinical routine and future research investigating the potential correlation of sCeAD and connective tissue disorder.

Acknowledgments

Funding: This study was supported by VASCage-Research Centre on Clinical Stroke Research. VASCage is a COMET Centre within the Competence Centers for Excellent Technologies (COMET) program and funded by the Federal Ministry for Climate Action, Environment, Energy,

Mobility, Innovation and Technology, the Federal Ministry of Labour and Economy, and the federal states of Tyrol, Salzburg and Vienna. COMET is managed by the Austrian Research Promotion Agency (Österreichische Forschun gsförderungsgesellschaft), FFG Project number: 898252. This study was also supported by the Austrian Science Fund (FWF): project P 29514-N32, to S.P. Jr.

Footnote

Conflicts of Interest: All authors have completed the ICMJE uniform disclosure form (available at https://qims.amegroups.com/article/view/10.21037/qims-23-1057/coif). All authors report that this study was supported by VASCage-Research Centre on Clinical Stroke Research. VASCage is a COMET Centre within the Competence Centers for Excellent Technologies (COMET) program and funded by the Federal Ministry for Climate Action, Environment, Energy, Mobility, Innovation and Technology, the Federal Ministry of Labour and Economy, and the federal states of Tyrol, Salzburg and Vienna. COMET is managed by the Austrian Research Promotion Agency (Österreichische Forschungsförderungsgesellschaft), FFG Project number: 898252. S.P. Jr reports the support from the Austrian Science Fund (FWF): project P 29514-N32. The authors have no other conflicts of interest to declare.

Ethical Statement: The authors are accountable for all aspects of the work in ensuring that questions related to the accuracy or integrity of any part of the work are appropriately investigated and resolved. The study was conducted in accordance with the Declaration of Helsinki (as revised in 2013). The study was approved by the institutional ethics committee of the Medical University of Innsbruck (EK#UN5072;325/4.1) and all patients provided appropriate informed consent.

References

1. Uhlig P, Bruckner P, Dittrich R, Ringelstein EB, Kuhlenbäumer G, Hansen U. Aberrations of dermal connective tissue in patients with cervical artery dissection (sCAD). J Neurol 2008;255:340-6.
2. Mayer-Suess L, Pechlaner R, Barallobre-Barreiro J, Boehme C, Toell T, Lynch M, Yin X, Willeit J, Gizewski ER, Perco P, Ratzinger G, Kiechl S, Mayr M, Knoflach M. Extracellular matrix protein signature of recurrent spontaneous cervical artery dissection. Neurology 2020;95:e2047-55.
3. Grond-Ginsbach C, Debette S. The association of connective tissue disorders with cervical artery dissections. Curr Mol Med 2009;9:210-4.
4. Giossi A, Ritelli M, Costa P, Morotti A, Poli L, Del Zotto E, Volonghi I, Chiarelli N, Gamba M, Bovi P, Tomelleri G, Carletti M, Checcarelli N, Meneghetti G, Morra M, Chinaglia M, De Giuli V, Colombi M, Padovani A, Pezzini A. Connective tissue anomalies in patients with spontaneous cervical artery dissection. Neurology 2014;83:2032-7.
5. Debette S, Goeggel Simonetti B, Schilling S, Martin JJ, Kloss M, Sarikaya H, et al. Familial occurrence and heritable connective tissue disorders in cervical artery dissection. Neurology 2014;83:2023-31.
6. Morris SA. Arterial tortuosity in genetic arteriopathies. Curr Opin Cardiol 2015;30:587-93.
7. MacCarrick G, Black JH 3rd, Bowdin S, El-Hamamsy I, Frischmeyer-Guerrerio PA, Guerrerio AL, Sponseller PD, Loeys B, Dietz HC 3rd. Loeys-Dietz syndrome: a primer for diagnosis and management. Genet Med 2014;16:576-87.
8. Loeys BL, Chen J, Neptune ER, Judge DP, Podowski M, Holm T, et al. A syndrome of altered cardiovascular, craniofacial, neurocognitive and skeletal development caused by mutations in TGFBR1 or TGFBR2. Nat Genet 2005;37:275-81.
9. Franken R, El Morabit A, de Waard V, Timmermans J, Scholte AJ, van den Berg MP, Marquering H, Planken NR, Zwinderman AH, Mulder BJ, Groenink M. Increased aortic tortuosity indicates a more severe aortic phenotype in adults with Marfan syndrome. Int J Cardiol 2015;194:7-12.
10. Morris SA, Orbach DB, Geva T, Singh MN, Gauvreau K, Lacro RV. Increased vertebral artery tortuosity index is associated with adverse outcomes in children and young adults with connective tissue disorders. Circulation

2011;124:388-96.
11. Mayer L, Boehme C, Toell T, Dejakum B, Willeit J, Schmidauer C, Berek K, Siedentopf C, Gizewski ER, Ratzinger G, Kiechl S, Knoflach M. Local Signs and Symptoms in Spontaneous Cervical Artery Dissection: A Single Centre Cohort Study. J Stroke 2019;21:112-5.
12. Mayer-Suess L, Geiger M, Dejakum B, Boehme C, Domig LM, Komarek S, Toell T, Kiechl S, Knoflach M. Sex-differences in psychosocial sequelae after spontaneous cervical artery dissection. Sci Rep 2022;12:611.
13. Yushkevich PA, Piven J, Hazlett HC, Smith RG, Ho S, Gee JC, Gerig G. User-guided 3D active contour segmentation of anatomical structures: significantly improved efficiency and reliability. Neuroimage 2006;31:1116-28.
14. Giossi A, Mardighian D, Caria F, Poli L, De Giuli V, Costa P, Morotti A, Gamba M, Gilberti N, Ritelli M, Colombi M, Sessa M, Grassi M, Padovani A, Gasparotti R, Pezzini A. Arterial tortuosity in patients with spontaneous cervical artery dissection. Neuroradiology 2017;59:571-5.
15. Touzé E, Southerland AM, Boulanger M, Labeyrie PE, Azizi M, Bouatia-Naji N, Debette S, Gornik HL, Hussain SM, Jeunemaitre X, Joux J, Kirton A, Le Hello C, Majersik JJ, Mocco J, Persu A, Sharma A, Worrall BB, Olin JW, Plouin PF. Fibromuscular Dysplasia and Its Neurologic Manifestations: A Systematic Review. JAMA Neurol 2019;76:217-26.

Cite this article as: Mayer-Suess L, Peball T, Pereverzyev S Jr, Steiger R, Galijasevic M, Kiechl S, Knoflach M, Gizewski ER, Mangesius S. Cervical artery tortuosity—a reliable semi-automated magnetic resonance-based method. Quant Imaging Med Surg 2024;14(2):1383-1391. doi: 10.21037/qims-23-1057

